J. Fluid Mech. (1978), *vol.* 88, *part* 2, *pp.* 223–240
Printed in Great Britain

Experiments on the dynamics of a gravity current head

By R. E. BRITTER AND J. E. SIMPSON

Department of Applied Mathematics and Theoretical Physics,
University of Cambridge

(Received 14 October 1977 and in revised form 14 February 1978)

Some of the dense fluid at the front of an advancing gravity current is observed to be mixed with the ambient fluid. This process continues when the cross-stream non-uniformities at the head of the current are suppressed by advancing the floor beneath the head. In the resulting two-dimensional flow regular billows are visible. This paper considers experimentally and analytically the inviscid gravity current head and specifically includes the observed mixing at the head. Experimental results were obtained with an apparatus in which the head of the gravity current was brought to rest by an opposing uniform flow. The mixing appears to occur through Kelvin–Helmholtz billows generated on the front of the head and controls the dynamics of the head. A momentum balance is used to analyse the flow and the problem is closed by quantitatively introducing the billow structure.

1. Introduction

The front part of a gravity current is deeper than the following steady flow and this raised section of the flow is referred to as the head of the gravity current (figure 1 (*a*), plate 1). When the gravity current is advancing over a rigid surface a three-dimensional unsteady flow field develops at the head which appears to be analytically intractable. The foremost part of the head consists of a complicated shifting pattern of lobes and clefts with an intermittent series of billows breaking away (Simpson 1969). However, solutions have been developed by Benjamin (1968) for the dynamics of the two-dimensional steady head of a gravity current in inviscid fluids. When we observe a gravity current advancing over a horizontal floor we see two processes not considered in Benjamin's inviscid analysis which we believe have some significance in the dynamics of the head. The first process is mixing between the two fluids at the upper interface of the head of the gravity current, the mixed fluid being left behind the advancing head. This requires that the velocity of advance of the head of a gravity current of constant depth (e.g. a one-dimensional inviscid gravity current on a horizontal surface) be less than the average velocity in the gravity current behind the head.

The second process is that in which fluid in front of the gravity current is overrun by the gravity current and then mixed within it (Allen 1971; Simpson 1972). This is a direct result of the no-slip condition imposed by the rigid surface. It was thought that an experiment in which velocity gradients at the boundary were small would be a useful test of Benjamin's analysis for the inviscid gravity current head. Attempts were made to reduce boundary velocity gradients by running gravity currents of fresh

water into ambient saline solutions, i.e. along a free surface, but it became apparent that, at least for laboratory scales, any impurities at the free surface resulted in the free surface acting as a no-slip surface. This effect was due, presumably, to significant surface-tension forces resulting from increased impurity concentration gradients along the surface ahead of the gravity current and the relatively small forces that are associated with gravity currents with small density differences. At larger scales or with large density differences the free surface might be expected to be a boundary with slip.

An alternative technique for suppressing the overrunning of the light fluid by the denser fluid is to reduce the relative velocity between the floor and the gravity current head to zero (Simpson 1972). This is the technique described in § 3 with the addition that the head of the gravity current is brought to rest by placing it in an opposing flow.

When the overrunning of less dense fluid is suppressed, the complicated lobe and cleft structure disappears and *regular* billows can be seen forming on the leading-edge slope of about 40°, rolling back above the head, and finally breaking down into a more random velocity and concentration field. Figure 1 (plate 1) shows shadowgraphs of gravity current heads brought to rest by means of an opposing flow. In figure 1 (*a*) the head is moving relative to the floor; mixing can be seen at the head and there are indications of a three-dimensional structure. The foremost point of the head (indicated by an arrow in figure 1 *a*) is raised above the floor. In figures 1 (*b*) and (*c*) the floor *beneath the denser fluid is fixed*, i.e. the relative velocity between the floor under the gravity current head and the foremost point of the gravity current head is zero, thereby reducing velocity gradients at the floor inside the gravity current head. In the latter examples the foremost point of the gravity current head is on the floor, the flow is nearly two-dimensional and more distinct billows can be seen. The behaviour of these flows is different from that of the familiar 'arrested saline wedge' described by Farmer (1951), Keulegan (1957) and Riddell (1970), in which a gentle, almost linear slope is seen, usually with no breaking waves. The difference appears to be associated with the existence of a boundary layer in the flow approaching the arrested saline wedge. The boundary layer, when contrasted with a uniform approach flow, will have smaller stagnation pressures near the ground and smaller velocity discontinuities (strictly, local velocity gradients) across the fluid/fluid interface. Both effects might explain the characteristics of an arrested saline wedge, i.e. the gentle slope and the absence of significant mixing across the interface.

In this paper we examine the behaviour of gravity current heads like those shown in figures 1 (*b*) and (*c*), in which the overrunning process has been suppressed. This is done by use of an apparatus in which the head is brought to rest by an opposing flow of less dense fluid arranged to have a uniform velocity profile. Figures 2 (*a*) and (*b*) show the difference between the production of these flows and of an 'arrested saline wedge'.

In essence, then, the paper considers, experimentally and analytically, the inviscid gravity current head of Benjamin complicated by the observed mixing of the two fluids at the head. A clearer understanding of this problem is a first step towards the solution of the problem of a gravity current advancing over a no-slip surface.

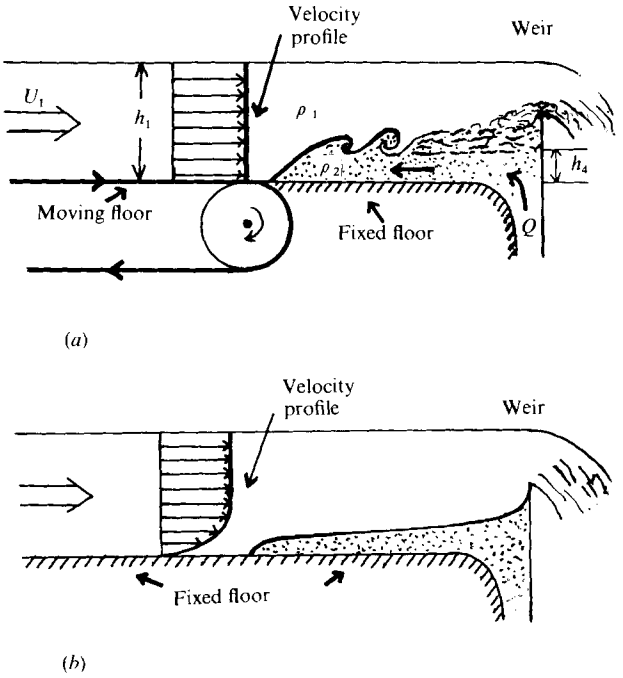

FIGURE 2. The production and effect of different incident velocity profiles. (*a*) Uniform velocity profile. (*b*) Boundary layer and arrested saline wedge.

2. Analysis

Consider the flow in the experimental arrangement depicted in figure 2(*a*), but where the velocity of the gravity current has not, as yet, been reduced to zero. U_1, Q, ρ_2, ρ_1, g and h_1 are the relevant independent variables, where Q is the volume flow rate of dense fluid per unit width of the channel. Introduction of the Boussinesq approximation reduces the independent variables to U_1, Q, g' and h_1, where

$$g' = g(\rho_2 - \rho_1)/\rho_1.$$

Interesting dependent variables are U_c, the velocity of the front in the experiment, and h_4, the depth of the dense fluid well behind the head, i.e. the depth of the following gravity current.

In dimensionless form

$$\frac{U_c}{U_1}, \frac{h_4}{h_1} = F_{1,2}\left(\frac{Qg'}{U_1^3}, \frac{U_1^2}{g'h_1}\right). \tag{2.1}$$

If the independent variables are now adjusted such that

$$\frac{U_c}{U_1} = F_1\left(\frac{Qg'}{U_1^3}, \frac{U_1^2}{g'h_1}\right) = 0 \tag{2.2}$$

then we expect, and observe, a unique (though not necessarily single-valued) relationship between $U_1^2/g'h_1$ and h_4/h_1. We present here an analysis that determines

$$U_1^2/g'h_1 = F_3(h_4/h_1) \tag{2.3}$$

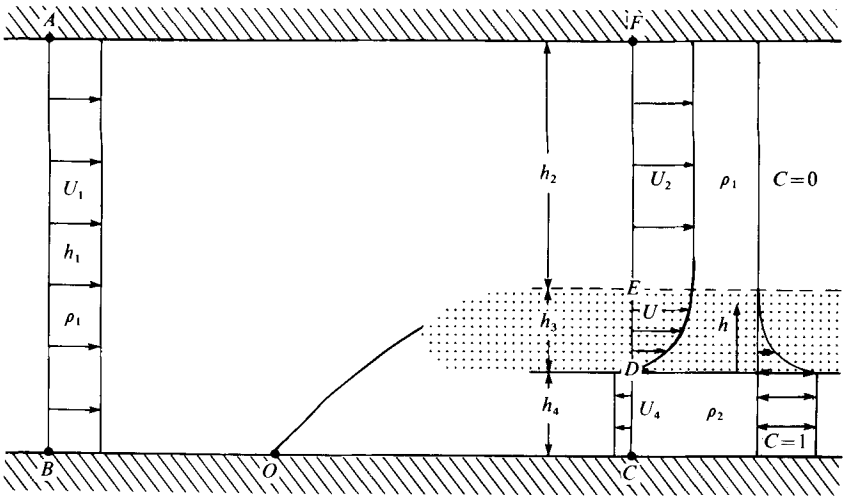

FIGURE 3. Physical model of the gravity current head observed in figures 1 (*b*) and (*c*).

for a given Qg'/U_1^3; then, with guidance from the experimental results, the controlling physical process is isolated, resulting in a further equation which allows a complete solution.

The analysis is restricted to miscible fluids or a flow in which the effects of surface tension may be neglected. Also the analysis is restricted to flows at Reynolds numbers high enough for an inviscid analysis to be adequate. The analysis is similar to Benjamin's except that another parameter, Q, the volume flow per unit width into the gravity current head of dense fluid (or the flow per unit width of dense fluid removed from the head as a result of mixing), is included. The flow observed in figures 1 (*b*) and (*c*) is represented by the model in figure 3, where the frame of reference is such that the head of the current is stationary.

The flow is inviscid, incompressible and steady. The upper and lower surfaces are rigid. Section AB is far enough upstream for the influence of the gravity current not to be felt. Section $CDEF$ is far enough downstream that all the velocities are horizontal and that the mixed region is not decreasing in thickness owing to its stable density stratification. However this section is not so far downstream that (i) mixing across the interface of which D is a member is significant, (ii) wave drag on the interface of which D is a member is significant and (iii) the mixed region has grown significantly in the manner of a decaying turbulent wake. The pressure at sections AB and $CDEF$ will be hydrostatic.

The downstream flow has been divided, somewhat arbitrarily, into three regions. The bottom region, of height h_4, is the flow into the gravity current head of the denser fluid, while the top region contains unmixed, less dense fluid. Between these is a third region, the collapsed wake from the billows, in which there is a velocity and a concentration profile. Thus uniform flow has been assumed everywhere except in the mixed region behind the head. This assumption will be poor as $(h_3+h_4)/h_1$ becomes small and its validity will be discussed in § 5.

Application of mass conservation to the two species gives

$$U_1 h_1 = U_2 h_2 + (\alpha - \beta) U_2 h_3 \tag{2.4}$$

and

$$-U_4 h_4 = \beta U_2 h_3 = Q, \tag{2.5}$$

where

$$\alpha U_2 h_3 = \int_0^{h_3} U(h)\,dh,$$

$$\beta U_2 h_3 = \int_0^{h_3} C(h)\,U(h)\,dh,$$

and $C(h)$ is the concentration of the denser fluid as a function of the distance h, where h is measured from the top of the lowest region. As the flow is steady, the net horizontal force external to and acting on the control volume $ABOCDEFA$ equals the net flux of horizontal momentum crossing the boundaries of the control volume. Arbitrarily setting the pressure at the stagnation point O to zero and introducing the Boussinesq approximation leads to

$$\tfrac{1}{2}U_1^2 h_1 + \tfrac{1}{2}g' h_1^2 + \tfrac{1}{2}U_4^2 h_1 = U_2^2 h_2 + Q(\delta\beta^{-1}U_2 - U_4) + \tfrac{1}{2}g'[h_2 + (1-\gamma)h_3]^2 + \tfrac{1}{2}g'(2\epsilon - \gamma^2)h_3^2, \tag{2.6}$$

where

$$\gamma h_3 = \int_0^{h_3} C(h)\,dh, \quad \delta U_2^2 h_3 = \int_0^{h_3} U^2(h)\,dh,$$

$$\epsilon h_3^2 = \int_0^{h_3} hC(h)\,dh.$$

When $Q = 0$ this reduces to

$$\tfrac{1}{2}U_1^2 h_1 - U_2^2 h_2 = -\tfrac{1}{2}g' h_1^2 + \tfrac{1}{2}g' h_2^2. \tag{2.7}$$

By combining (2.4)–(2.6), we may write

$$F_4\left(\frac{U_1^2}{g'h_1}, \frac{h_4}{h_1}, \frac{Qg'}{U_1^3}, (\alpha, \beta, \gamma, \delta, \epsilon)\right) = 0, \tag{2.8}$$

or, subject to specifying the wake profiles, easily obtain

$$U_1^2/g'h_1 = [F_5(h_4/h_1)]_{Qg'/U_1^3 = \text{const}}$$

by a simple iterative technique. A solution in the above form is not convenient in the limit $h_4/h_1 \to 0$ because in this limit $U_1^2/g'h_4$ becomes indeterminate. Therefore (2.8) was manipulated into the form

$$F_6\left(\frac{U_1^2}{g'h_4}, \frac{h_4}{h_1}, \frac{Qg'}{U_1^3}, (\alpha, \beta, \gamma, \delta, \epsilon)\right) = 0.\dagger \tag{2.9}$$

When $q = Qg'/U_1^3 = 0$,

$$f = U_1^2/g'h_4 = (2-\phi)(1-\phi)/(1+\phi),$$

where $\phi = h_4/h_1$, a result obtained by Benjamin (1968, equation 2.22). Solutions to

$$\dagger\ f - 2fx(1+\xi)^2 - 2\delta\beta^{-1}qf^2\phi x(1+\xi) - 2q^2f^3\phi + q^2f^3 + \left\{1 + \frac{\gamma B}{1+B\phi}(1-\phi)\right\}\left\{2 - \phi - \frac{\gamma B\phi}{1+B\phi}(1-\phi)\right\} + \frac{B^2\phi}{x^2}(\gamma^2 - 2\epsilon) = 0, \tag{2.9a}$$

where

$$f = U_1^2/g'h_4, \quad \xi = (1-\alpha/\beta)qf\phi, \quad \phi = h_4/h_1, \quad B = qf/\beta(1+\xi),$$
$$x = (1+B\phi)/(1-\phi), \quad q = Qg'/U_1^3.$$

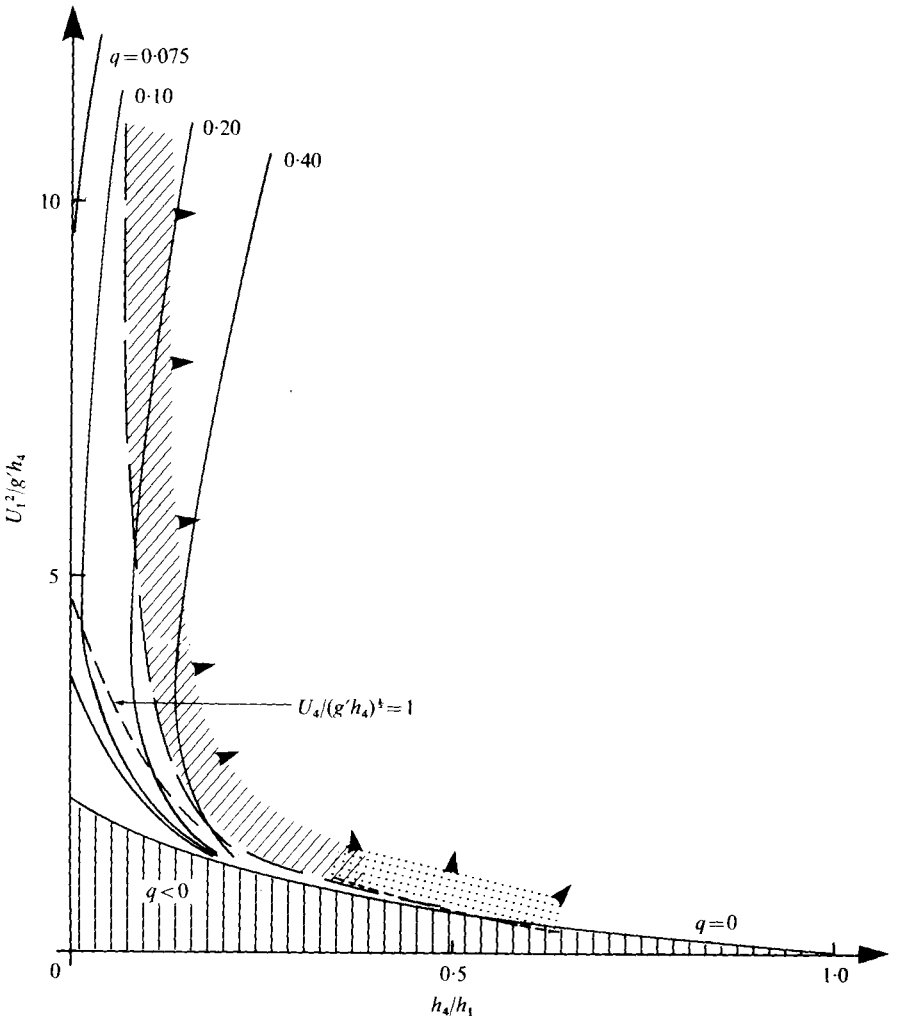

FIGURE 4. Analytical results for $U_1^2/g'h_4$ as a function of h_4/h_1 and the non-dimensional volume flux $q = Qg'/U_1^3$. The shaded areas indicate non-physical solutions: ||||, $q < 0$; ////, $h_2 < 0$; ⁝⁝⁝, region of net energy gain. The arrowheads indicate a continuation of the shaded areas.

(2.9a) were obtained (for typical wake parameters, see § 4) and those for $U_1^2/g'h_4$ are shown in figure 4. The *form* of the curves in figure 4 is not sensitive to variations in the values of the wake parameters.

In addition to the two obvious regions of unphysical solutions ($U_1^2/g'h_1 < 0$ and $h_4/h_1 < 0$), a region for which h_2 is negative may be determined and one for which there is a net energy gain. This last region is determined by evaluating the fluxes of kinetic and potential energy crossing the boundaries of the control volume and the work done by the forces at the boundaries of the control volume. These regions have been included in figure 4, where the arrowheads indicate extensions of the shaded areas.

We also note that if the flow sketched in figure 2(a) is not to be controlled by the source configuration (our experiments indicated it was not) then the characteristic

velocity of long waves relative to the head must be zero or to the right. If there is no mixed region such a constraint may be written as

$$U_2^2/g'h_2 + U_4^2/g'h_4 \leqslant 1.$$

That is $U_4/(g'h_4)^{\frac{1}{2}} \leqslant A$, where A is a function of h_4/h_1, with a maximum of 1 at $h_4/h_1 = 0$. We have neglected the mixed layer immediately above the dense layer in this argument so the limit is better expressed as $U_4/(g'h_4)^{\frac{1}{2}} \leqslant A = O(1)$.

A curve of the solutions for which $U_4/(g'h_4)^{\frac{1}{2}} = 1$ is included in figure 4. Solutions below this line are those for which $U_4/(g'h_4)^{\frac{1}{2}} < 1$. If we impose this constraint the region of physically possible solutions is seen to be very limited.

The analysis presented here is for a flow with a rigid upper surface but the experiments to be described in §§ 3 and 4 were made with the experimentally simpler configuration of a free surface. Analysis of flow with a free surface introduces both a new variable, the total depth, and a new equation, Bernoulli's equation along the free surface. Benjamin (1968) has shown that inclusion of the new variable and new equation modifies the solution by a factor $1 + O((\rho_2 - \rho_1)/\rho_1)$. In the experiments described in §§ 3 and 4 the maximum variation in the total depth of the flow was estimated to be less than 0·1 %, i.e. less than 0·01 cm, a variation that was not measureable in the present apparatus. The authors agree with Benjamin (1968) that 'The corrections $O((\rho_2 - \rho_1)/\rho_1)$ ... are unlikely to be significant in the interpretation of experiments using salt water ....'

3. Apparatus and procedure

The apparatus used for these measurements was designed and built when one of the authors (J.E.S.) was working at the University of Reading. The purpose was to study the behaviour of the head of a gravity current in conditions as near as possible to a steady state. To achieve this, a steady current of water was pumped through the working section, the floor of the tank was moved in the form of an endless belt, and a saline flow was introduced at one end.

In the experiments to be described here, which involved suppressing the usual ingestion of fluid beneath the nose which arises when the nose advances relative to the floor, the head was brought to rest on the fixed part of the floor close to the end of the moving belt. With a constant rate of input of saline solution in any one experiment, it was found possible to bring the head to rest for a certain value of U_1, the speed of both the opposing flow and the conveyor belt.

This apparatus is shown schematically in figure 5. The exposed length of the conveyor belt is just under 1 m and the height h_1 of the water flow can be varied between 6 and 12 cm. The available range for U_1 was between 1 and 6 cm s^{-1}.

The input of the channel flow and that of the saline underflow are monitored by rotameter flowmeters, and the floor speed has been calibrated in terms of the voltage supplied to the driving motor. The channel flow passes through a flow straightener 1·5 cm long consisting of a mesh of hexagonal cells of width 0·3 cm. The vertical variation of U_1 was less than ± 2 % in an experiment and any turbulence was of low intensity (estimated to be less than $\frac{1}{2}$ %). For the observations described here other measurements required were the shape and external dimensions of the gravity current. These were made from shadowgraphs produced by a 300 W slide projector, 3·5 m

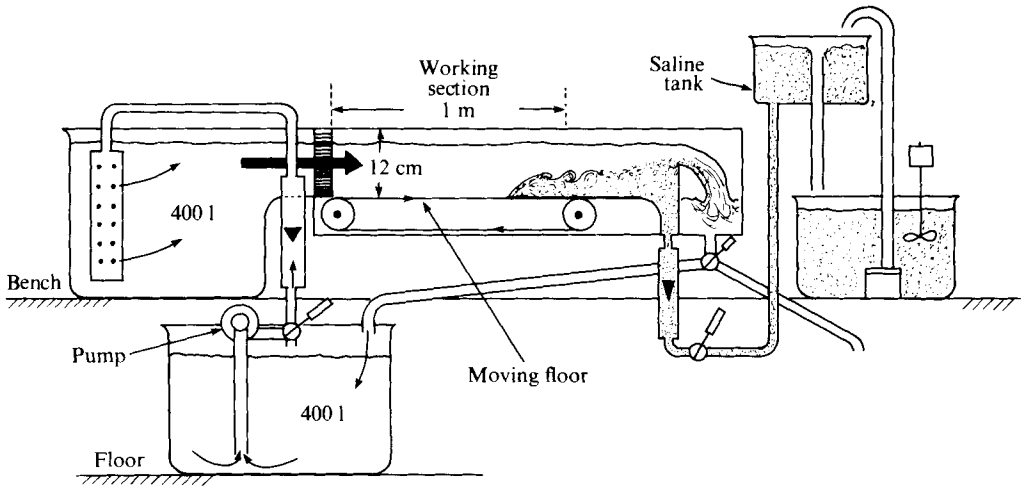

FIGURE 5. Schematic diagram of apparatus.

distant, which shone from the rear of the tank and formed an image on a tracing panel in front of the tank.

The range of salt concentrations used was from $\frac{1}{2}$ to 4 %. By 1 % we mean 1 % by weight of added salt: the actual value of $(\rho_2-\rho_1)/\rho_1$ depends on the temperature, and for a 1 % solution is about 0·0076 at 20 °C.

During a run, which typically lasted up to about 20 min, the rate of saline input was usually kept constant. After the pump and floor speeds had been changed it was necessary to wait for up to a minute before a new steady opposing flow rate was attained; this was shown by velocity measurements with a heated thermistor probe. When a steady state had been reached with the head within 1 cm from the end of the fixed floor, either a photograph was taken or the height of the top of the head and that of the following steady flow (h_4) were marked on the tracing paper on the front of the tank. Figures 1 (*b*) and (*c*) show photographs of typical heads brought to rest in this way.

The value of h_4 was measured to the nearest millimetre from the shadowgraph display, giving a maximum error of 10 % in the small flows (0·5 cm) reducing to 2·5 % in the deeper flows. The total depth h_1 could be measured to within 1 %.

Two other depths were measured. The total head height was estimated as the height of the top of the billows before they began to break up and lose their clear outline. The depth of the mixed layer (defined as the mean depth over which fine structure was observed) was also measured, but to within the experimental accuracy, this was equal to the height of the top of the billows above the dense layer. That is, the depth from the floor to the top of the billows and the depth from the floor to the top of the mixed layer were equal; this depth is referred to as the total head height h_3+h_4.

The volume flow was measured with the saline rotameter, and should be accurate to within 10 %. However, it is not certain that all this volume flow reaches the head, some being lost owing to mixing behind the head near the weir, and measurements were made to determine what proportion actually reached the front. For a large volume flow a smaller fraction actually reached the front of the gravity current and was mixed there. Using the velocity of injected dye particles we obtained a corrected

volume flux, per unit width of the tank. The experimental error in the non-dimensional volume flux $q = Qg'/U_1^3$ is estimated to be $\pm 30\,\%$.

Further checks confirming the velocity measurements were obtained from the study of the streaklines produced when aluminium particles were injected into the flow and photographed over intervals of $\frac{1}{4}$ or $\frac{1}{8}$ s with illumination over a slit about 2 cm wide down the centre of the channel.

Measurements were made of the velocity and salinity profiles in the mixed region behind the head, in order to determine the forms of the profiles $U(h)$ and $C(h)$ to be used in the analysis. The velocity and salinity profiles were obtained at a distance of $10h_4$–$20h_4$ behind the foremost point of the head. Owing to the limited size of the apparatus it was not possible to determine whether the profiles varied significantly downstream.

Mean velocity measurements were made using a DISA hot-film probe with a DISA constant-temperature anemometer. Care was taken to reduce the error due to temperature sensitivity of the probe. Mean velocities were accurate to within 5 % for velocities greater than 1 cm s^{-1}. Mean salinity measurements were made with a conventional conductivity meter based on the design of the Hydraulic Research Station at Wallingford, England. These measurements are accurate to within 5 % also.

4. Experimental results

The analysis as presented in § 2 requires two empirical inputs and the first experiments were directed towards determining these inputs. The required inputs are the form of the velocity and salinity profiles in the mixed layer and the non-dimensional volume flux $q = Qg'/U_1^3$ of the denser fluid carried forward into the head and mixed with the less dense fluid there. There is no requirement that these parameters be independent of the fractional depth h_4/h_1, although it was not expected that the form of the velocity and salinity profiles would be a strong function of the fractional depth. Measurements were obtained in the range $0{\cdot}03 \leqslant h_4/h_1 \leqslant 0{\cdot}25$.

The velocity and salinity profiles in the mixed layer are well fitted by

$$1 - \frac{U(h)}{U(h_3)} = \left(1 - \frac{h}{h_3}\right)^m, \quad \frac{C(h)}{C(0)} = \left(1 - \frac{h}{h_3}\right)^n,$$

where $m = 4 \pm 0{\cdot}5$ and $n = 4 \pm 0{\cdot}5$. At small values of h_4/h_1 the profiles were better fitted with $m = 4$ and $n = 5$, however the inaccuracy of the mean velocity and salinity measurements themselves, the inaccuracy of the determination of the extent of the mixed region and the difficulty in maintaining a steady flow over long periods all combined to hide any definite variation of the form of the profiles with the fractional depth h_4/h_1. Inclusion of an empirical variation of the wake profiles with h_4/h_1 is thought to be an unnecessary complication when the analysis is based on a simple model. Therefore the values $m = 4$ and $n = 4$ have been used to determine the wake parameters in the analysis of § 2.

The other required empirical input, q, had a mean value, obtained from all our measurements, of $0{\cdot}11 \pm 0{\cdot}04$ (i.e. $\pm$ one standard deviation). However, q tended to increase with h_4/h_1 from $0{\cdot}075 \pm 0{\cdot}025$ at $h_4/h_1 \simeq 0{\cdot}05$ to $0{\cdot}15 \pm 0{\cdot}05$ at $h_4/h_1 \simeq 0{\cdot}20$.

The result of most interest in the present experiments is U_1, the velocity of the oncoming flow required to hold the head of the gravity current steady, or alternatively

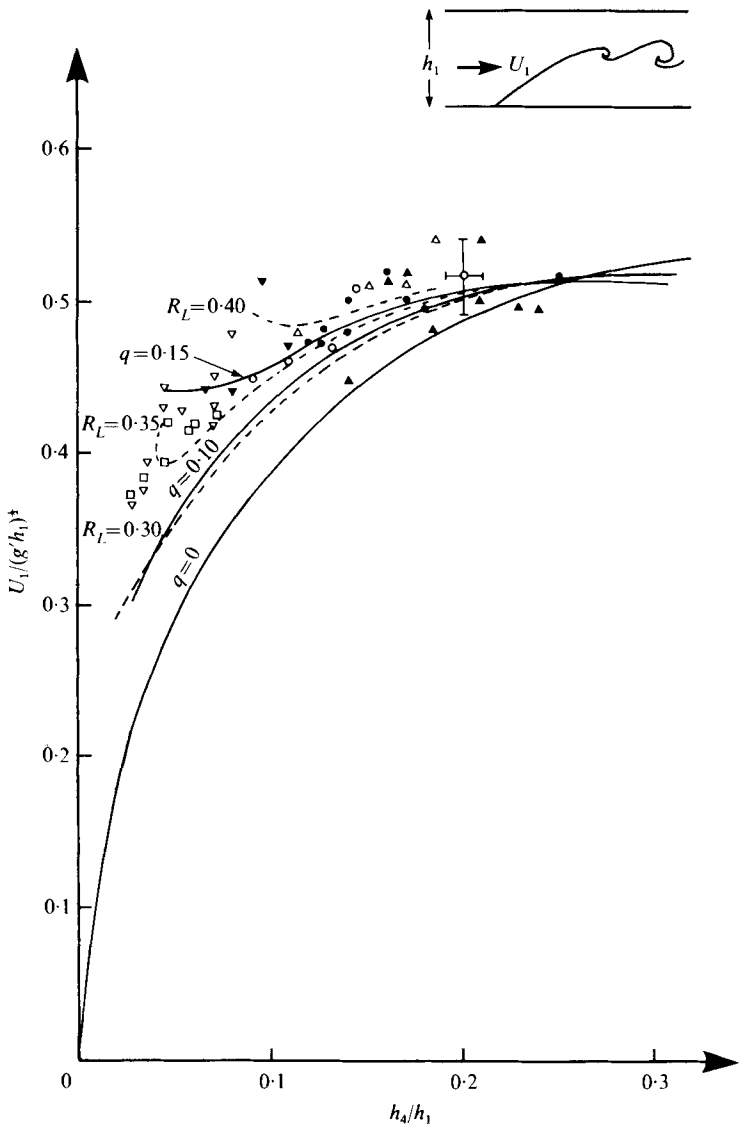

FIGURE 6 (*a*). For legend see next page.

the velocity of advance of the gravity current head into stationary surroundings. Two methods of non-dimensionalizing this velocity are available: the velocity may be scaled on the total depth of the ambient fluid to form the Froude number $U_1/(g'h_1)^{\frac{1}{2}}$ or the velocity may be scaled on the depth of the following gravity current to form the Froude number $U_1/(g'h_4)^{\frac{1}{2}}$. These two Froude numbers are shown as functions of the fractional depth h_4/h_1 in figures 6 (*a*) and (*b*) respectively and compared there with results from the analysis of § 2 for values of the non-dimensional mass flux q of 0, 0·10 and 0·15. The curves labelled R_L = 0·30, 0·35 and 0·40 may be ignored until § 5. The curves labelled q = 0 correspond to the results deduced by Benjamin (1968) for a gravity current with no mixing at the head. The mixing at the head of the gravity current increases the predicted Froude numbers considerably above those expected

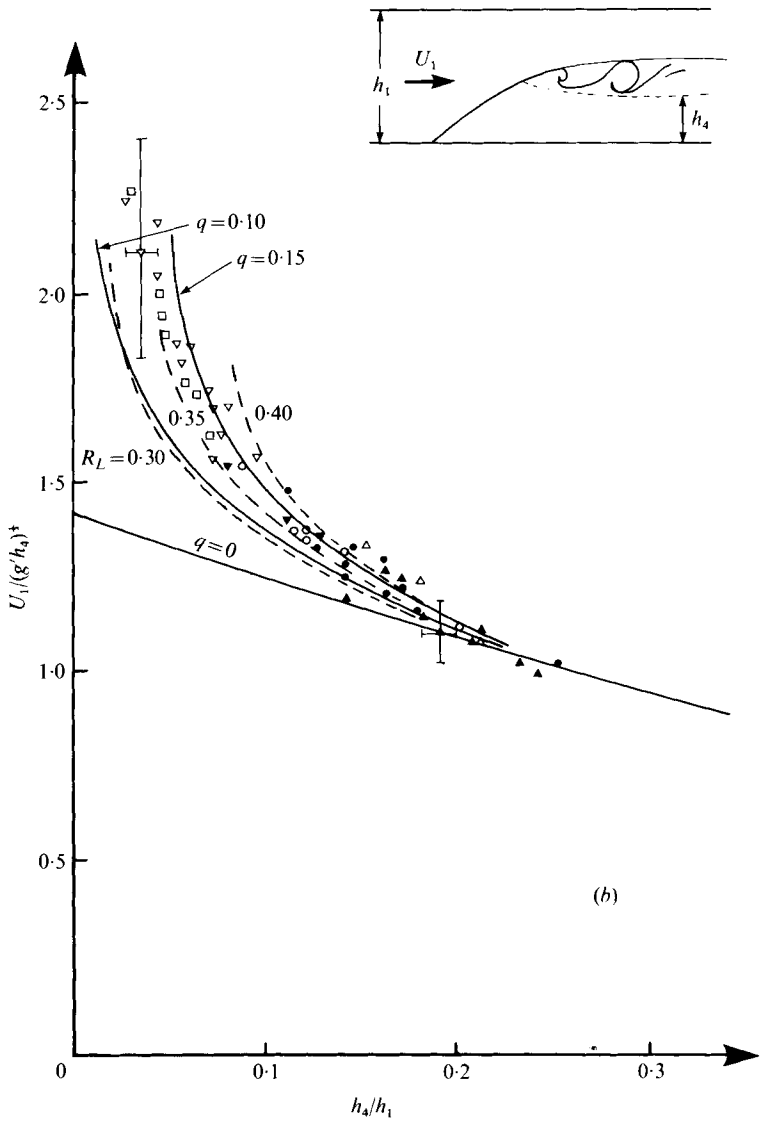

FIGURE 6. Graphs of (*a*) $Fr = U_1/(g'h_1)^{\frac{1}{2}}$ and (*b*) $Fr = U_1/(g'h_4)^{\frac{1}{2}}$ against h_4/h_1. ——, analytical values for different non-dimensional volume fluxes q; – – –, analytical values for different values of $R_L = g'h_3/(\Delta U)^2$ (see § 5). Values of $(\rho_2-\rho_1)/\rho_1$: △, 0·0037; ○, 0·0074; ▽, 0·015; □, 0·030. Open symbols, $0{\cdot}04 < q < 0{\cdot}10$; solid symbols, $0{\cdot}10 \leqslant q < 0{\cdot}21$.

in the absence of mixing. The experimental results are generally in agreement with the analysis presented in § 2 for q between 0·10 and 0·15, consistent with our separate measures of q.

It should be noted that the maximum value of $U_1(g'h_4)^{\frac{1}{2}}$ measured was 2·25, i.e. well in excess of the maximum value of $2^{\frac{1}{2}}$ given by Benjamin (1968), but see § 5 for further consideration of this point.

In co-ordinates which have the less dense fluid stationary (i.e. for a gravity current head advancing into stationary surroundings) the velocity of the following gravity current is $U_1 + U_4$, or $U_1(1 + U_4/U_1)$. Therefore an inviscid, non-entraining, gravity

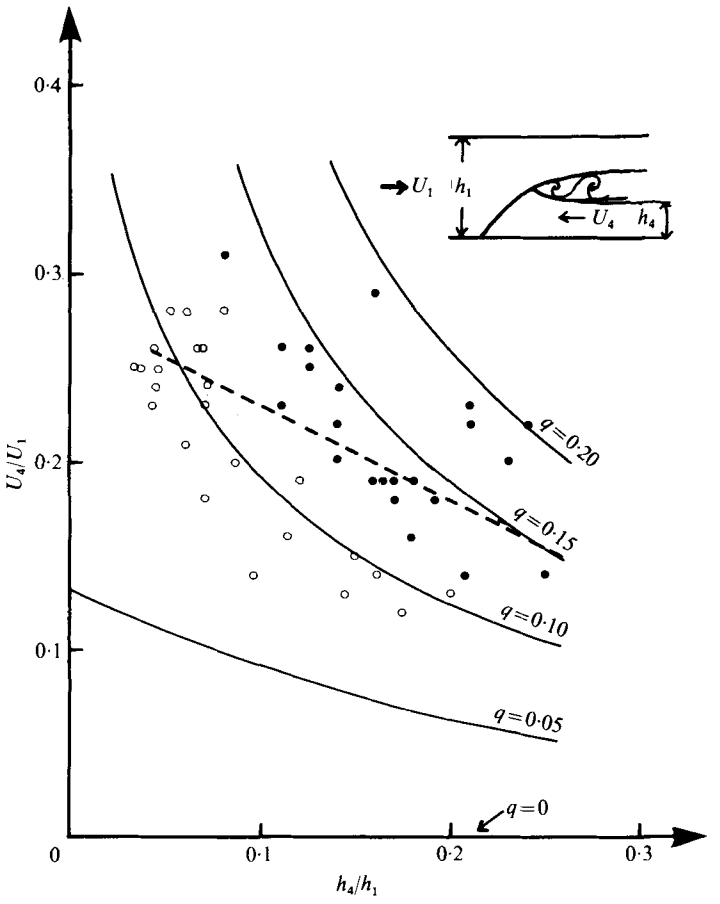

FIGURE 7. Graph of U_4/U_1 against h_4/h_1. ——, values for different non-dimensional volume fluxes q; – – –, straight line of least-squares difference. ○, $q < 0{\cdot}10$; ●, $q > 0{\cdot}10$.

current of constant depth on a horizontal plane preceded by a gravity current head will have a Froude number

$$\frac{U_1}{(g'h_4)^{\frac{1}{2}}}\left(1+\frac{U_4}{U_1}\right)$$

and the flux at any cross-section will be $U_1 h_4(1+U_4/U_1)$. It therefore becomes apparent that the ratio of the 'overtaking' velocity U_4 $(=Q/h_4)$ to the opposing velocity U_1 is an important variable in determining the velocity of the gravity current head when only the flux in the following gravity current is specified. This ratio U_4/U_1 is plotted in figure 7 as a function of the fractional depth h_4/h_1 and compared there with results from the analysis of § 2. The experimental data show general agreement with the analysis for q in the range 0·10–0·15. The least-squares linear fit to the data is in excellent agreement with the observed variation of q with fractional depth h_4/h_1. The ratio U_4/U_1 is only a weak function of h_4/h_1, increasing at smaller values of h_4/h_1. The mean of the measured values was $0{\cdot}22 \pm 0{\cdot}04$. The Froude number of the following gravity current has a maximum value in the present experiments of

$$\frac{U_1}{(g'h_4)^{\frac{1}{2}}}\left(1+\frac{U_4}{U_1}\right) = 2{\cdot}25\,(1+0{\cdot}25) = 2{\cdot}81,$$

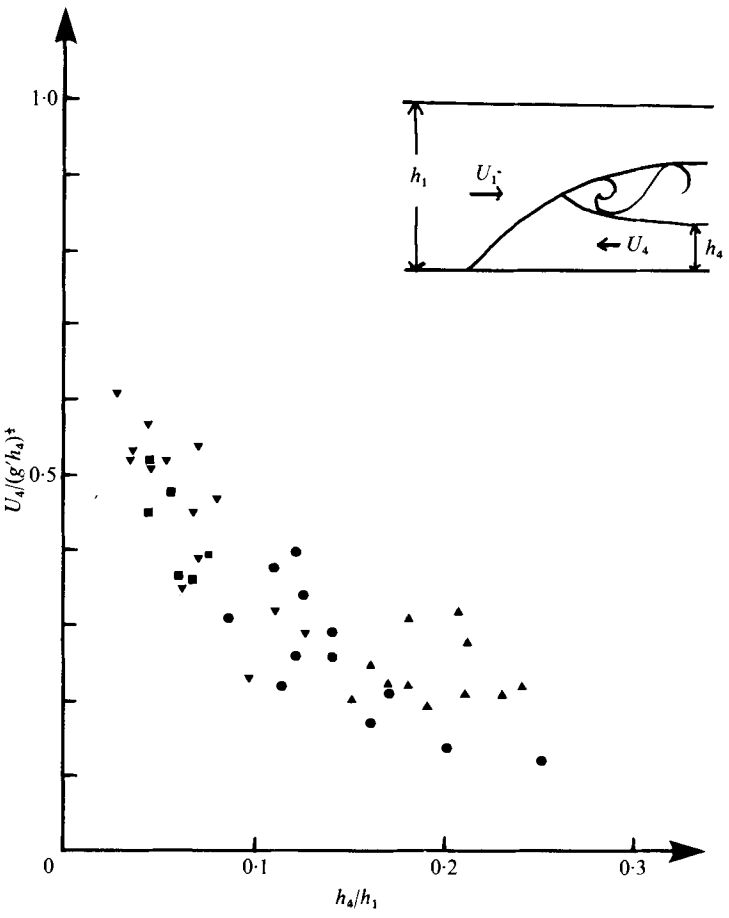

FIGURE 8. Graph of $U_4/(g'h_4)^{\frac{1}{2}}$ against h_4/h_1. Values of $(\rho_2-\rho_1)/\rho_1$: ▲, 0·0037; ●, 0·0074; ▼, 0·015; ■, 0·0030.

approximately twice that predicted in the absence of mixing at the gravity current head (i.e. $2\frac{1}{2}$).

The 'overtaking' velocity U_4 may also be non-dimensionalized with the 'overtaking' layer depth to form the variable $U_4/(g'h_4)^{\frac{1}{2}}$. Arguments were presented in § 2 to suggest that $U_4/(g'h_4)^{\frac{1}{2}} \leqslant A$, where A is of order unity when $h_4/h_1 \to 0$, and that it decreases as the fractional depth h_4/h_1 is increased. $U_4/(g'h_4)^{\frac{1}{2}}$ is plotted in figure 8 as a function of h_4/h_1 and indeed $U_4/(g'h_4)^{\frac{1}{2}} < O(1)$ and increases as h_4/h_1 decreases. Extrapolation of the data in figure 8 to $U_4/(g'h_4)^{\frac{1}{2}}$ equals $O(1)$ or possibly 1 at $h_4/h_1 = 0$ is not unreasonable and this will be discussed further in § 5.

The gravity current head shown in figures 1(*b*) and (*c*) has the form of a wedge-shaped region of dense fluid with a maximum included angle of $40° \pm 5°$ at the apex (which is also the stagnation point in the frame of reference which holds the head stationary). The interface between the fluids was less steep away from the apex and finally became nearly horizontal. Small waves could be seen some way up the interface slope, travelling up the slope. These grew rapidly in amplitude, rolling up into discrete billows containing the two fluids and being convected away over the following gravity current. The billows initially grew in a coherent, two-dimensional manner but

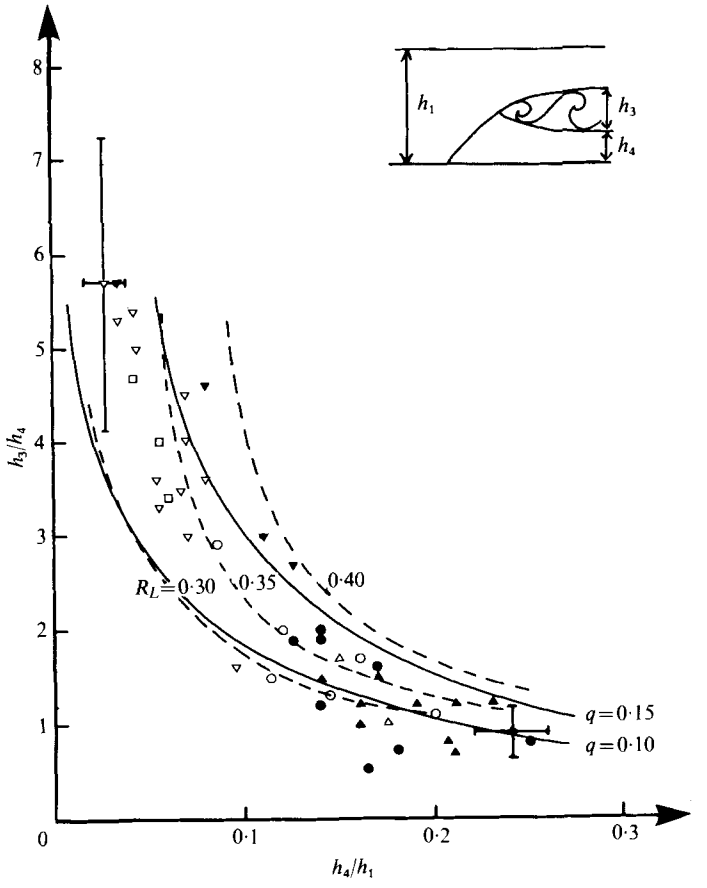

FIGURE 9. Graph of head height h_3/h_4 against h_4/h_1. Symbols and curves as in figure 6.

eventually were disrupted by the appearance of fine-scale turbulence possibly due to their own gravitational instability. The resulting disorganized fine-scale turbulence was also convected away over the following gravity current to form the mixed region considered in the analysis. It was observed that the maximum size to which the billows grew was equal to the size of the mixed region behind the head. That is, even though the coherent billow structure collapsed, the extent of the mixed region did not.

The height h_3 of the mixed region behind the head non-dimensionalized with h_4 is shown in figure 9 to increase sharply as $h_4/h_1 \to 0$, reaching $5{\cdot}7 \pm 1{\cdot}6$ at $h_4/h_1 = 0{\cdot}03$. This is much larger than the value of approximately 1 often quoted for the head height of gravity currents advancing over no-slip surfaces (Keulegan 1957, 1958), although the comparison is not strictly valid as previous experiments (on gravity currents advancing over no-slip surfaces) have either not recognized h_4/h_1 to be an important variable or have obtained data at $h_4/h_1 \simeq 0{\cdot}2$. The calculated values of h_3/h_4 for values of q of 0·10 and 0·15 are also plotted in figure 9 and show good agreement with the experimental results.

The appearance of the growth of individual billows at the gravity current head suggested that the growth may be a finite amplitude Kelvin–Helmholtz instability resulting from the velocity discontinuity across the fluid interface.

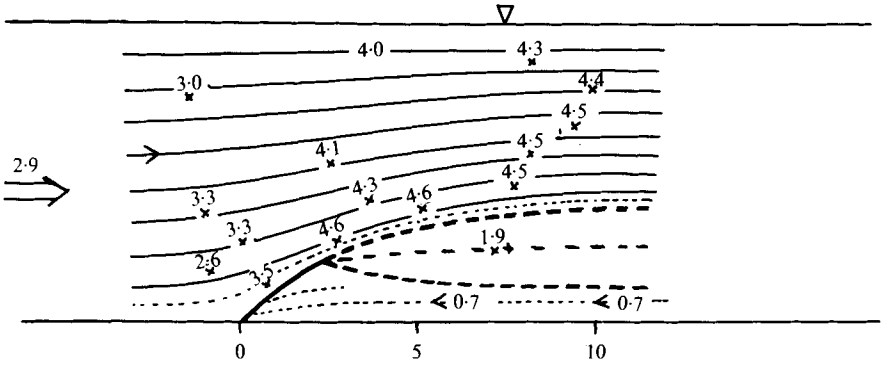

FIGURE 10. Velocity flow field near gravity current head as measured from tracer particles. $(\rho_2-\rho_1)/\rho_1 = 0{\cdot}0037$, $h_4/h_1 = 0{\cdot}12$.

The growth of individual billows may be quantified by $(\Delta U)^{-1}da/dt$, where a is the width of the billow normal to the locus of the billow centre and ΔU is the velocity difference across the shear layer. In our experiments the relevant ΔU is difficult to determine, however we have taken $\Delta U = U_m - U_4$, where U_m is the velocity near the interface at the point where the billows start to form. This point is also difficult to determine and we have taken it to be the intersection between the wedge-shaped profile of the dense fluid and the line drawn through the billow centres, which was approximately horizontal. Direct measurements of U_m and the velocity field outside the gravity current head were obtained with aluminium tracer particles for three different values of the fractional depth h_4/h_1. These suggested that U_m/U_1 is constant at $1{\cdot}55 \pm 0{\cdot}10$ for all $h_4/h_1 \leqslant 0{\cdot}25$. The data for $h_4/h_1 = 0{\cdot}12$ are shown in figure 10 and this pattern is similar to the others measured. It is also to be noted in figure 10 that the velocity difference across the mixed region is approximately the same as that across the interface at the supposed origin for billow growth. The billow convection velocity is included in figure 10 and was observed to be the mean of the velocities either side of the density interface: a not surprising result.

At small times the non-dimensional billow growth rate $(\Delta U)^{-1}da/dt$ was estimated as $0{\cdot}21 \pm 0{\cdot}05$, $0{\cdot}26 \pm 0{\cdot}05$ and $0{\cdot}24 \pm 0{\cdot}05$ for $h_4/h_1 = 0{\cdot}22$, $0{\cdot}12$ and $0{\cdot}06$. This is similar to the growth rate for a homogeneous shear layer, where $(\Delta U)^{-1}da/dt = 0{\cdot}19$ (Brown & Roshko 1974), implying a very small initial Richardson number across the shear layer (i.e. a very thin region of velocity and density variation). The density interface is continually renewed and will therefore be very sharp, while the region of velocity variation, though Reynolds number dependent, is such that we estimate the initial gradient Richardson number in our experiments to be less than $0{\cdot}01$.

In any one experiment the billows grew to a fixed size before becoming indistinct amongst the turbulent fine structure. Measurements made from ciné films of experiments with $h_4/h_1 = 0{\cdot}22$, $0{\cdot}12$ and $0{\cdot}06$ showed that the maximum billow size was attained at a non-dimensional time of $g't/\Delta U \simeq 3$. The non-dimensional height of the mixed region after the collapse of the billow structure was found to be constant, independent of h_4/h_1 and g', at $g'h_3/(\Delta U)^2 = 0{\cdot}33 \pm 0{\cdot}08$ (48 observations). It would be more apt to non-dimensionalize the mixing layer in terms of the velocity difference across the mixed region itself but this, as shown above, is approximately equal to ΔU. That is, the parameter $g'h_3/(\Delta U')^2$, where $\Delta U'$ is the velocity difference across

the mixed layer, is also approximately constant at 0·33 and has the nature of a layer Richardson number. The ratio of the maximum billow amplitude to the billow wavelength was found to be $0{\cdot}8 \pm 0{\cdot}2$ independent of g' and h_4/h_1. The final layer Richardson number and the ratio of the maximum amplitude to the wavelength of the billows are consistent with the results of Thorpe (1973) for the Kelvin–Helmholtz instability between fluids of different density when the initial gradient Richardson number is small.

5. Discussion and conclusions

Experimental investigation of a gravity current head with the lobe and cleft structure (and associated overrunning of one fluid by the other) suppressed indicates that the leading interface of the gravity current head is subject to an instability similar, both qualitatively and quantitatively, to the Kelvin–Helmholtz instability of a shear layer separating two fluids of different density as described by Thorpe (1973). At the head of a gravity current advancing over a no-slip surface the shifting pattern of lobes and clefts makes analysis of the dynamics of the head more complicated, however examination with slit lighting has shown the presence of similar billows involved in the mixing (Simpson 1969). An analysis (which is no more than a momentum balance) is presented that adequately describes the experimental observations. However, the analysis does not, by itself, give a unique solution. Recognizing that the instability and mixing at the head constitute the mechanism controlling the flow and have the nature of the Kelvin–Helmholtz instability allows an *a priori* description of the mixing. The experiments of Thorpe (1973) suggest that the parameter

$$R_L = g'h_3/(\Delta U)^2$$

(our notation) is constant and equal to $0{\cdot}35 \pm 0{\cdot}1$. The results of Thorpe might lead us to expect that R_L as defined above might be constant in the present experiments however it is probably fortuitous that the numerical constants in the two experiments are so close, the experimental configurations being considerably dissimilar. Nevertheless, constraining our solution to (2.9*a*) to satisfy $R_L = g'h_3/(\Delta U)^2 = 0{\cdot}35$ (suggested by Thorpe's results) leads to a unique solution. This solution is included in figure 6 and, as expected, good agreement is observed. The present results cover the range $0{\cdot}03 \leqslant h_4/h_1 \leqslant 0{\cdot}25$. It was not possible in these experiments to obtain flows with $h_4/h_1 > 0{\cdot}25$. This upper limit to the realizable fractional depths is similar to, but less than, that of 0·35 anticipated by Benjamin (1968).

The experimental results are surprising in that the interesting limit $h_4/h_1 = 0$ is very difficult to approach. At the smallest value of h_4/h_1 observed ($h_4/h_1 = 0{\cdot}03$), the ratio h_3/h_1 is still approximately constant at 0·24. That is, the flow when $h_4/h_1 = 0{\cdot}03$ is significantly different from the case of the gravity current in an infinitely deep fluid ($h_4/h_1 = 0$). Similarly the Froude number $U_1/(g'h_1)^{\frac{1}{2}}$ is approximately 0·4 at $h_4/h_1 = 0{\cdot}03$ and, assuming that U_1 is independent of h_1 as h_1 becomes very large, must fall to zero at $h_4/h_1 = 0$.

Consider the case when h_4/h_1 is vanishingly small in more detail. The analysis of § 2 (which assumed uniform flow everywhere other than in the mixed region) leads to

$$q^2f^3 - f(1 - 2\gamma\beta^{-1}q) + 2 = 0 \tag{5.1}$$

when $h_4/h_1 = 0$. The assumption of uniform flow is poor in this limit. However, an alternative analysis† which assumes only that the velocities at great heights are independent of the existence of the current leads to precisely the same equation

$$q^2f^3 - f + 2(1 + \gamma h_3/h_4) = 0, \tag{5.2}$$

where the ratio h_3/h_4 is determined to be qf/β when $h_4/h_1 = 0$. The only physical solutions are those with f and q non-negative. As q is increased above zero f has two roots (corresponding to $q^2f^3 \gtrless 1$), then a double root and finally no roots, except that for $q = 0$ the equation has the one trivial solution $f = 2$ obtained by Benjamin (1968). Benjamin noted that if there was mixing at the head then $U_1^2/g'h_4 = 2$, where h_4 must be taken as the 'densimetric mean level of the disturbed interface'. Thus, in the present notation,

$$U_1^2/g'(h_4 + \gamma h_3) = 2.$$

This result is a good approximation to the data in figure 6(*b*) when the fractional depth is small. It is simply shown that at the double root

$$q^2f^3 = 1 \quad \text{and} \quad f = 3(1 - 2\gamma\beta^{-1}q)^{-1},$$

The relation $q^2f^3 = 1$ is equivalent to $U_4^2/g'h_4 = 1$; that is, in the frame of reference that holds the head stationary, the inflow at the back of the gravity current has a Froude number of 1 and the maximum volume flow rate Q is carried forward to the head for a gravity current of depth h_4.

There are no solutions to (5.2) when

$$3q^{\frac{2}{3}} + 2\gamma\beta^{-1}q > 1, \tag{5.3}$$

so for wake profiles with $m = 4$ and $n = 4$ (taken from experiments with $h_4/h_1 \geqslant 0{\cdot}03$), $\gamma/\beta = 2{\cdot}25$ and $q_{\max} = 0{\cdot}089$. It was noted in § 4 that, experimentally, q varied from $0{\cdot}15 \pm 0{\cdot}05$ at $h_4/h_1 \simeq 0{\cdot}20$ to $0{\cdot}075 \pm 0{\cdot}025$ at $h_4/h_1 \simeq 0{\cdot}05$. Extrapolation of the experimental results to $h_4/h_1 = 0$ with $q \leqslant 0{\cdot}089$ appears to be possible. Thus, with the constraints $U_4/(g'h_4)^{\frac{1}{2}} \leqslant 1$ and $q \leqslant 0{\cdot}089$, the maximum value of $U_1/(g'h_4)^{\frac{1}{2}}$ at $h_4/h_1 = 0$ is 2·24, at $q = 0{\cdot}089$. As the maximum value of $U_1/(g'h_4)^{\frac{1}{2}}$ observed is $2{\cdot}25 \pm 0{\cdot}3$, at $h_4/h_1 = 0{\cdot}03$, we expect that the relevant solution to (5.2) is that for $q = q_{\max}$ and is the double root. Alternatively, the experimentally determined parameter $R_L = g'h_3/(\Delta U)^2 = 0{\cdot}33 \pm 0{\cdot}08$ could be extrapolated to $h_4/h_1 = 0$ and a solution obtained, however a small error in our estimate of R_L may lead to no solutions. Nevertheless R_L is calculated to be 0·25 for the double root. If the wake profiles are characterized by $m = 4$ and $n = 5$ when $h_4/h_1 = 0$ then $R_L = 0{\cdot}32$ at the double root and we have further support for the conjecture that the double root is the physically relevant one.

The velocity field inside the gravity current head has not been studied in detail but it is reported here that the slope of the front of the head was $40 \pm 5°$. This was less than the expected slope of 60° (von Kármán 1940).

We have shown in this paper that the mixing between the two fluids at the head of a gravity current is an important process in determining the dynamics of a gravity current head and that an analysis incorporating this mixing is possible. The next

† We assume hydrostatic pressure on AB (figure 3) and FC, apply Bernoulli's equation along BO and CO and take A and F to great heights.

stage in the study of gravity current heads must include the consequences of a no-slip lower boundary: the elevation of the foremost point of the gravity current head and the ingestion of fluid beneath it. Numerous experiments on gravity currents advancing into still water, but with a fractional depth not very different from 0·2 (Keulegan 1958; Yih 1965; Barr 1967), have shown that the Froude number $U_1/(g'h_4)^{\frac{1}{2}}$ is approximately equal to 1 and also that the height ratio $h_3/h_4 \simeq 1$. Preliminary experiments have been made in which the range of fractional depths has been much extended and various opposing flows have been applied. These show large variations in the Froude number and in the head height similar to those seen in this investigation.

In conclusion we reiterate the comment in the introduction that, although this study was initially undertaken as a first step towards understanding gravity currents advancing over a no-slip surface, we believe that it has direct relevance to gravity currents running at free surfaces in the absence of any significant surface-tension forces.

This apparatus was originally constructed at the University of Reading by Mr M. Cantwell and Mr R. Flatt, who worked out the details of the design. We are grateful to them for their interest in the project and their ingenuity in overcoming difficulties. It was later transferred to Cambridge and modified there. J.E.S. thanks especially Dr J. R. Milford for helpful discussions in the early stages and the Natural Environment Research Council for a grant to support the work. R.E.B. is supported by a grant from Shell, Thornton Research Centre. The authors express their thanks to Dr P. F. Linden for his encouragement.

REFERENCES

ALLEN, J. R. L. 1971 Mixing at turbidity current heads, and its geological implications. *J. Sediment. Petrol.* **41**, 97–113.

BARR, D. I. H. 1967 Densimetric exchange flow in rectangular channels. III. Large scale experiments. *Houille Blanche* **22**, 619–631.

BENJAMIN, T. B. 1968 Gravity currents and related phenomena. *J. Fluid Mech.* **31**, 209–248.

BROWN, G. J. & ROSHKO, A. 1974 On density effects and large structure in turbulent mixing layers. *J. Fluid Mech.* **64**, 775–816.

FARMER, H. G. 1951 An experimental study of salt wedges. *Woods Hole Oceanographic Inst. Rep.* no. 51–99.

KÁRMÁN, T. VON 1940 The engineer grapples with non-linear problems. *Bull. Am. Math. Soc.* **46**, 615–683.

KEULEGAN, G. H. 1957 Form characteristics of arrested saline wedges. *U.S. Nat. Bur. Stand. Rep.* no. 5482.

KEULEGAN, G. H. 1958 The motion of saline fronts in still water. *U.S. Nat. Bur. Stand. Rep.* no. 5831.

RIDDELL, J. C. 1970 Densimetric exchange flow in rectangular channels. IV. Arrested saline wedge. *Houille Blanche* **25**, 317–330.

SIMPSON, J. E. 1969 A comparison between laboratory and atmospheric density currents. *Quart. J. Roy. Met. Soc.* **95**, 758–765.

SIMPSON, J. E. 1972 Effects of the lower boundary on the head of a gravity current. *J. Fluid Mech.* **53**, 759–768.

THORPE, S. A. 1973 Experiments on instability and turbulence in a stratified shear flow. *J. Fluid Mech.* **61**, 731–751.

YIH, C.-S. 1965 *Dynamics of Non-homogeneous Fluids*, p. 137. Macmillan.

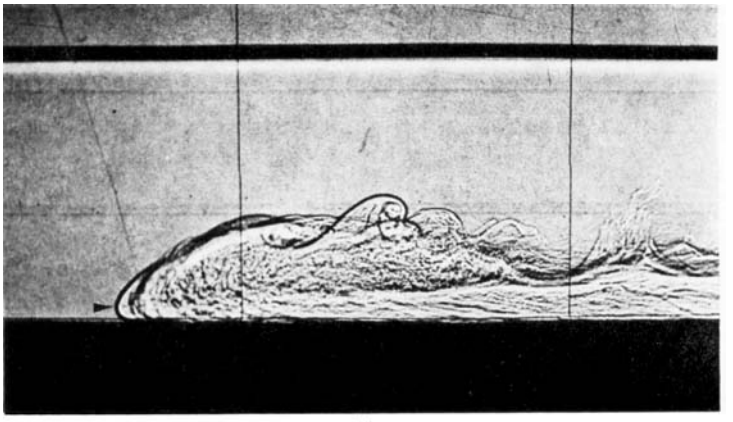

(*a*)

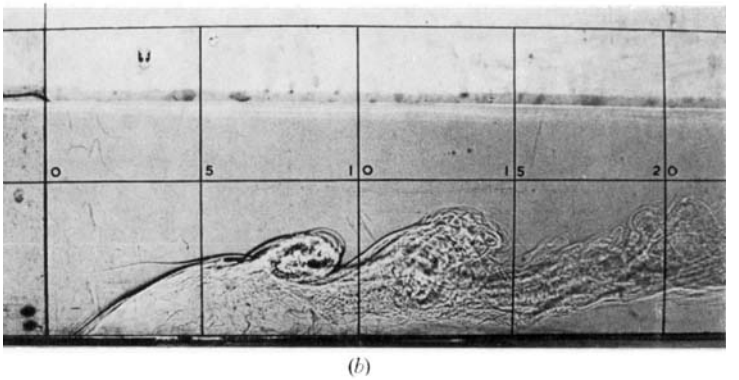

(*b*)

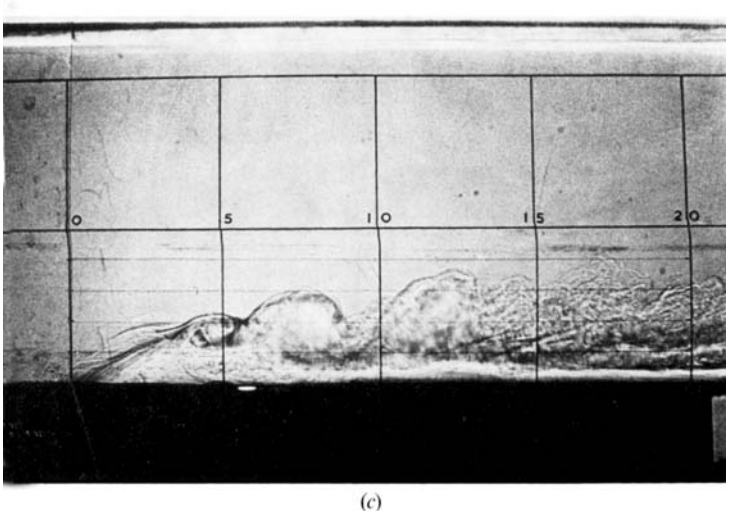

(*c*)

FIGURE 1. Shadowgraphs of gravity current heads brought to rest by an opposing flow with uniform velocity profile. (*a*) Whole floor moving at the same velocity as the opposing flow. The arrow indicates the elevation of the foremost point of the gravity current. $(\rho_2-\rho_1)/\rho_1 = 0{\cdot}0074$, $h_4/h_1 = 0{\cdot}13$. (*b*) With a fixed floor beneath the dense fluid. $(\rho_2-\rho_1)/\rho_1 = 0{\cdot}0037$, $h_4/h_1 = 0{\cdot}19$. (*c*) With a fixed floor beneath the dense fluid. $(\rho_2-\rho_1)/\rho_1 = 0{\cdot}015$, $h_4/h_1 = 0{\cdot}04$.